A Thesis

entitled

Evaluating the Dosimetric Accuracy of Small Gating Windows in Radiotherapy

by

Wesley A. Short

Submitted to the Graduate Faculty as partial fulfillment of the requirements for the Masters of Science Degree in Biomedical Science in Medical Physics

Dr. Nicholas Sperling, Committee Chair

Dr. Ishmael Parsai, Committee Member

Dr. Diana Shvydka, Committee Member

Dr. Amanda Bryant-Friedrich, Dean
College of Graduate Studies

The University of Toledo

May 2018

An Abstract of

Evaluating the Dosimetric Accuracy of Small Gating Windows in Radiotherapy

by

Wesley A. Short

Submitted to the Graduate Faculty as partial fulfillment of the requirements for the Masters of Science Degree in Biomedical Science in Medical Physics

The University of Toledo
May 2018

Cancers in the abdomen and thorax present increased difficulties for successful treatment because they exhibit large amounts of internal movement due to a patient's respiratory cycle. In order to manage respiratory motion, several methods are currently being used clinically including gating. In gated radiotherapy, the beam is selectively turned on when the lesion is inside the desired treatment window and the beam is turned off when the lesion moves outside the treatment window. The accuracy of small gating windows combined with VMAT is of interest because the beam is turned on for short periods of time and gantry must ramp up speed often and quickly. Small gating windows can theoretically decrease the volume of normal tissue being irradiated because the degree of movement is significantly less over the small fraction of the respiratory cycle.

The dosimetric accuracy of small gating windows was evaluated with two static phantoms: a commercially available diode array with a micro-ionization chamber for isocenter point dose measurements, and a custom cylindrical acrylic phantom wrapped with radiochromic film. Five clinically accepted VMAT plans were delivered using a Varian Edge. The measured dose was compared with the planned dose for five beam-on configurations: 100%, 70%, 50%, 30%, and 20%. A programmable phantom was used to generate the gating signal for 15 BPM in combination with the Varian RPM system. The gamma analysis was used to compare the measured

dose with the planned dose using a 1%/1 mm, 0.5%/0.5 mm, and 1% dose difference criteria for the diode array and 3%/3 mm criteria for the radiochromic film.

The max deviation from the 100% beam-on delivery was 1.8, 0.8, and 1.3% for the 1mm/1%, 0.5mm/0.5%, and 1% DTA. Average point deviations were slightly higher than the 100% beam-on delivery and deviated the most compared to the expected dose for the two large gating windows, but the small gating windows were slightly less than the 100% beam-on delivery. Treatment time increased by an average factor of 7 for the small gating window (20%). 100% beam-on delivery had the lowest passing rates for the radiochromic film with a general increase in passing rates as the gating window became progressively smaller.

Data supports the use of small gating windows on a Varian Edge, suggesting there is minimal difference between gating levels. However, clinical treatment times are significantly longer, which may lead to an increase of intra-fraction patient motion.

Acknowledgments

I would like to thank my advisor, Dr. Nicholas Sperling, for his guidance and support through my research and education. I would also like to thank Dr. Ishmael Parsai, Dr. David Pearson, and Dr. Diana Shvydka for guiding me in my educational and clinical journey. I also wish to thank my colleagues, family, and my wife, Leah, for their support and encouragement over the years.

Contents

List of Tables

List of Figures

List of Abbreviations

4D	Four Dimensional
6FFF	6 Mega Voltage nominal energy photon beam flattening filter free
10FFF	10 Mega Voltage nominal energy photon beam flattening filter free
ABC	Active-breathing control
ASCII	American Standard Code for Information Interchange
BEV	Beams Eye View
BPM	Breaths per Minute
cm	centimeter
CT	Computed Tomography
DD	Dose Difference
DIBH	Deep Inspiration Breath Hold
DICOM	Digital Imaging and Communications in Medicine
DTA	Distance to Agreement
EEBH	End Expiration Breath Hold
FFF	Flattening Filter Free
Gy	Gray
HD-MLC	High-Definition Multileaf Collimator
IMRT	Intensity-Modulated Radiation Therapy
Linac	Linear accelerator
MV	Mega Voltage

mm	millimeter
NTCP	Normal Tissue Complication Probability
OAR	Organ at Risk
OD	Optical Density
PTV	Planning Target Volume
QA	Quality Assurance
RPM	Real-Time Position Management
SBRT	Stereotactic Body Radiation Therapy
SSD	Source to Surface Distance
VMAT	Volumetric Modulated Arc Therapy

Chapter 1

Introduction

Success in radiation therapy is dependent upon accurate tumor localization while minimizing normal tissue damage. Abdominal and thoracic tumors, particularly near the diaphragm, present increased complexity due to tumor motion with patient respiration. In order to account for this motion, physicians have had to expand their target volumes to encompass the entire range of motion of the tumor; however, the movement of the tumor through the phases of patient respiration leads to an increase in the volume of normal tissue treated.

1.1 Respiratory Management Techniques

Several motion management techniques have been routinely employed to manage lesion movement including breath hold techniques, forced shallow-breathing, and gated radiotherapy. Although other techniques for the management of tumor motion have also been implemented such as tumor tracking, they are much less commonly implemented.

Breath hold techniques such as deep inspiration breath hold (DIBH) or end expiratory breath hold (EEBH) are increasingly implemented for treatment of abdominal, thoracic, and breast cancers. DIBH has become increasingly common for breast cancer, especially patients with cancer of the left breast, because it pulls the heart

inferiorly and posteriorly away from the chest wall decreasing the later cardiac complications [19]. It also increases the lung tissue volume leading to dosimetry advantages that may be exploited. Breath hold treatments may be carried out through assisted breathing methods or patient voluntary breath hold techniques.

Active Breathing Control (ABC) is implemented by Elekta through the use of Active Breathing Coordinator. ABC is an assisted breath hold technique where the respiratory signal is measured with a digital spirometer. An operator initiates the system where a balloon valve, connected with the spirometer, is inflated assisting the patients breath hold. Treatment is performed only during the assisted breath hold. Multiple published studies have demonstrated the effectiveness of ABC in reducing the normal tissue dose and reproducibly minimizing tumor motion for many lesion sites [4, 17, 18, 25].

Real-Time Position Management (RPM) (Varian Medical Systems) is a video-based system to record breathing cycles that may be used for free breathing and breath hold protocols. Correlation of patient external anatomy and tumor motion through the respiratory phases allows treatment of lesions where motion management is of concern. Workflow for clinics implementing the Varian RPM system is outlined in the American Association of Physicists in Medicine (AAPM) Task Group Report 76 [8]. An infrared camera tracks reflective markers on a box positioned on the patients external surface generating a waveform that will be used for corresponding with internal lesion movement. During treatment, the beam is automatically interrupted when the patients breathing falls outside the desired treatment range.

EEBH is another method of breath-hold more commonly used for abdominal lesions. With EEBH, the lung volume is decreased which increases the volume below the diaphragm. EEBH has been shown to improve the position reproducibility over DIBH with reproducibility of less than 0.4 mm and 1.3 mm for EEBH and DIBH respectively, and a larger fraction of the patients respiratory cycle of 42% occurs within

25% of the range of average exhale position with respect to 15% of the average inhale position [2]. While reproducibility improvements and respiratory windows are beneficial for EEBH over DIBH, the ability of the patient to maintain a breath hold at exhalation is diminished over breath holds performed during inhalation. More EEBH breath holds must be performed for a given treatment carried out with DIBH. Breath hold techniques have been effectively demonstrated to reduce margins and improve treatment outcomes, particularly for stereotactic radiotherapy.

First developed for stereotactic body radiation therapy (SBRT), forced shallow breathing via abdominal compression limits the motion of lesions through the use of a compression plate positioned over the patients abdomen. Several studies have evaluated abdominal compression for limiting intra-faction motion with mixed results. Wunderink et al. report that abdominal compression can be effectively used for lesions in the liver and treatment course reproducibility was never significantly greater than treatment planning [26]. Bouilhol et al. report that abdominal compression did not improve tumor motion significantly for upper and middle lobe lesions of the lung and lower lobe lesions still need to be evaluated on a case-by-case basis; however, Negoro et al. showed compression can be used to reduce the lesion movement from a range of 8 to 20 mm down to a range of 2 to 11 mm [3, 12]. Abdominal compression may be useful in limiting tumor motion, but it needs to be evaluated on a case-by-case basis for radiotherapy patients.

Gated radiotherapy is another motion management technique, and the focus of this investigation, that refers to treatments were the beam is selectively turned on when the tumor is in a desired window for treatment. The window is the open part of the beam, as defined by the MLC, that will be used to treat the target volume. When the lesion moves outside the window for treatment, the beam is turned off until the lesion moves back into the planned window. Gated radiotherapy does not actively tract the moving lesion, rather, the motion of the lesion is correlated with the respiratory

motion being tracked. Gated radiotherapy allows for smaller internal margins because the gating window is selectively chosen to correspond to respiratory phases exhibiting relatively little target motion. Subsequently, the planning target volume (PTV) may be decreased, limiting the normal tissue receiving prescription dose. Gated treatments can decrease the normal tissue complication probability (NTCP) or allow for dose escalation with an identical NTCP. Tracking may be performed by two common methods: external markers and internal fiducial markers. The Varian RPM external marker system is the most widely used system. A box with reflective markers is positioned on the patients skin and a camera measures the motion via reflected light from an infrared illuminator [5]. The breathing movement is correlated with the reflective marker movements, and analysis of the motion is used to trigger and pause the radiation during treatment delivery. Throughout the remainder of this report, small gating windows refer to treatments performed with low beam-on duty cycles (i.e. 20% or 30% beam-on deliveries). Large gating windows will refer to longer beam-on duty cycles that are typically encountered with gated radiotherapy such as 70% beam-on times.

1.2 Patient Specific Quality Assurance

Advanced treatment modalities have paved the way for highly conformal treatments that deliver high doses to the target while minimizing the normal tissue dose received. As such, the need for quality assurance (QA) to verify the patient treatment delivery is magnified. Several methods exist for patient specific QA methods including: true composite, perpendicular field-by-field, and perpendicular composite. Each can be carried out with many different phantoms: ionization chambers, diode arrays, radiochromic film, electronic portal imaging devices (EPIDs), and gel phantoms.

The true composite method allows for simultaneous sampling of all relevant treat-

ment parameters including: MUs, gantry, collimator, couch angles, jaw, and MLC positions [11]. Film, paired with an ionization chamber, has typically been used for this method, but new diode arrays including the ArcCheck (Sun Nuclear Corporation) and Delta4 (ScandiDos) have allowed for true composite absolute dose measurements. The main advantages mentioned in Miften et al. include: the ability to detect inaccuracies in all relevant treatment parameters, the resultant dose distributions closely resemble the actual patient dose distributions, and the ability to only analyze one dose image [11]. Using film, this method may not detect errors if the film is not crossed by portions of the beam; however, the 3D diode arrays mentioned above allow for sampling of the entire beam [11]. The true composite method should be implemented whenever possible, but angular dependence of detectors may inhibit its practical implementation. Perpendicular field-by-field is recommended in this situation.

In this method, a fixed gantry angle is used for each treatment field individually. Planar diode arrays include the MapCheck (Sun Nuclear Corporation) or the Octavius 729 (PTW) to name a few, but film has also been used with this method. The principle advantage with this method is that each field may be analyzed individually [11]. By measuring a composite, an underdosage due to one field may be averaged out with an overdosage due to a second field; current software for 3D phantoms (ArcCheck, Delta4, etc.) allow for measurements of each beam making it a true field-by-field, in turn, the perpendicular method should only be used when angular dependence is of significant concern. This perpendicular method may also be performed as a composite (perpendicular composite) meaning it can be performed faster, but potential errors may go unnoticed and its implementation should not be used.

Methods to carry out plan verification QA include ionization chambers, diode arrays, radiochromic film, EPIDs, and gel phantoms. Ionization chambers allow for plan-verification at a single point. Several 2D and 3D phantoms have inserts that allow for the insertion of a micro-ionization chamber for single-point dose measure-

ments. This method is also very valuable for film dosimetry where the ionization chamber is used to measure the absolute dose and the film obtains the dose distribution measurements. Because of the finite chamber volume, placement of the ionization chamber should be in a relatively uniform region of the dose distribution to limit the volume averaging effect. Gel dosimeters provide a high-resolution method for intensity-modulated radiation therapy (IMRT) dose verification, and they have other clinical applications including in-vivo dosimetry and verification of secondary devices in the clinic. A thorough literature review on gel dosimeters has been published by Yoichi et al. with a few brief highlights mentioned here [23]. Readout of gel dosimeters is accomplished with magnetic resonance imaging, optical-CT, or x-ray CT with optical-CT yielding the most accurate readout modality. Accuracy of gel dosimeters can achieve 5% uncertainty with 95% confidence, and, while not as accurate as standard methods, it is still accurate enough for many clinical applications. [23]. The limiting factor for routine clinical implementation is the expense; the long term expenses can exceed two or three times that of routine devices including 3D diode arrays. Further improvements in gel dosimeters may make them increasingly common for future applications.

Diode arrays and radiochromic film are two very common QA methods with diode arrays exceedingly surpassing the use of radiochromic film. Radiochromic film has been used clinically for several decades and comes with different applications in mind such as machine QA or patient specific QA. They do not require the use of developer solutions and dark rooms like their predecessor. Use of film for absolute dosimetry requires a calibration curve to plot the relationship between dose and optical density. Several advantageous features of radiochromic film are the high spatial resolution, the large dynamic dose range, their low energy dependence over the clinical range, and their near tissue equivalence. The angular dependence exhibited by radiochromic film is only about 1-2% with angles approaching parallel [24]. Radiochromic film un-

dergoes a color change that is proportional to absorbed dose which is determined by measuring the optical density (OD) of the film seen in equation 1.1.

$$OD = log_{10}(\frac{I_o}{I}) \tag{1.1}$$

For absolute dosimetry, a dose response curve (calibration curve) must be obtained for each lot of film. A known dose is delivered to the film, and the net optical density is measured. Radiochromic film is insensitive to visible light, but it is sensitive to ultraviolet light. One disadvantage of radiochromic film is the post-irradiation stabilization time. Uncertainties with stabilization may be minimized by allowing six hours (minimum) for polymerization stabilization with twenty-four hours being recommended [24]. Commercially available diode arrays have been available for several years including the MapCheck, ArcCheck, and the Delta4. Their ease of use is the greatest advantage diode arrays present. Unlike film dosimetry, immediate knowledge of the verification plan quality is known with diode arrays, whereas, radiochromic film requires the stabilization time period. Many articles have been published characterizing commercially available diode arrays. Diode arrays have limited dose rate dependence and low energy dependence for MV beams but, unfortunately, can suffer from angular dependence.

Comparison of measured dose distributions with planned distributions have historically been accomplished via several methods: isodose distribution superimposition, dose profiles, dose difference (DD) calculations, distance to agreement (DTA), and the gamma analysis. Superimposing isodose lines is a qualitative method for quickly identifying localized dose differences; however, a quantitative method typically needs to be used for final approval. Dose profiles across a distribution can be used to visualize the degree of discrepancy between the planned distribution and the measured.

DD and DTA are two commonly used quantitative measures to evaluate the agree-

ment of planned and measured dose distributions. The overall concept of DD and DTA has been presented by Harms et al. [6]. DD looks at a point in the dose distribution and compares it to the corresponding measured point and determines if it falls within the pre-defined clinically acceptable criteria of 2% or 3% typically. DD is overly sensitive to high dose gradient regions because corresponding points may suffer large differences from relatively minor misalignments. These large dose differences are often clinically insignificant [6]. On the other hand, DTA is more accurate in high dose gradient regions, but it suffers in low dose gradient regions, unlike DD. DTA is the distance between a measured dose point and the point in the measured dose distribution containing the same dose level. For shallow dose gradients, points with matching dose levels may be great distances apart leading to a failed DTA; however, the dose difference between them relatively small. In an effort to correct the pitfalls of each system, a composite analysis was developed by Harms et al. [6]. In the composite analysis, each point is evaluated to determine if the pre-determined criteria are exceeded for the DD and DTA. If a point fails both, it is identified on a composite distribution. The composite distribution is a binary distribution and ultimately displays the dose difference. The absence of an index measuring the calculation quality also severely limits the composite analysis [10].

Low et al. formalized an evaluation technique to simultaneously analyze DD and DTA called the gamma index [10]. Equation 1.2 shows the gamma distribution as presented by Low et al.,

$$\gamma(r_m) = min\{\Gamma(r_m, r_c)\}\forall\{r_c\} \tag{1.2}$$

$$\Gamma(r_m, r_c) = \sqrt{\frac{r^2(r_m, r_c)}{\Delta d_M^2} + \frac{\delta^2(r_m, r_c)}{\Delta D_M^2}} \tag{1.3}$$

where d_M is the DTA criterion, D_M is the dose difference criterion, $r(r_m,r_c)$ is the distance from the evaluated (TPS calculated point) point to the reference (measured)

point, and (r_m,r_c) is the difference between the evaluated and the reference doses [10]. For gamma distributions that evaluate greater than unity, the calculation fails and vice versa. The composite analysis presented by Harms et al. was limited by the absence of a numerical metric to measure the calculation quality, but the gamma distribution calculation is not limited in the same manner and a quality index may be presented. The initial publication by Low et al. only involve one-dimensional, but the authors further developed the gamma distribution for two-dimensional measurements that are in widespread clinical use with radiochromic film and diode arrays [9].

1.3 Literature Review

Numerous studies have been published on the use of gating for the treatment of lesions exhibiting high degrees of respiratory motion. The combination of volumetric modulated arc therapy (VMAT) and gating significantly increases the complexity of treatments and necessitates the need for dose verification that has also been investigated by several authors.

Noto et al. compared five breath-hold periods with an uninterrupted VMAT plan and analyzed the pass rates for a 1% dose difference measured with a 2-D diode array [14]. Using a Synergy linac (Elekta AB) five VMAT plans (three liver and two lung) were measured with a MatriXX Evolution (IBA Dosimetry) positioned inside the MULTICube (IBA Dosimetry) plastic water phantom and a PTW 30013 Farmer ion chamber [14]. Diode arrays allow for efficient dose verification. Beam-on times of 10, 15, 20, 30, and 40 seconds were used to simulate breath-holds with manual interrupts of 5 seconds and were compared with the uninterrupted delivery. Noto et al. reported isocenter dose deviations of 0.5, 0.2, 0.2, 0.0, and 0.0% for beam-on times of 10, 15, 20, 30, and 40 seconds respectively with differences not being statistically significant [14]. 1% DD pass rates were 85, 99.9, 100, 100, and 100% for the same order [14].

Using small breath-hold windows decreased the delivery reproducibility when delivered from an Elekta Synergy linac. With free-breathing gated treatment delivery, the beam-off remains in an active beam hold state where the next beam-on delay is insignificant; however, this study evaluated short breath-holds where the beam was manually interrupted-meaning the beam was no longer in an active state so there was a noticeable beam-on delay. Patients only being able to maintain short breath holds are not likely ideal candidates for breath-hold treatments where a beam-on delay would result from the stand-by state. The authors attribute the dose deviation to a transient period for gantry speed rise after an interrupt where a dose rate adjustment may provide more accurate performance, thereby, reducing the dose contribution during the transient period to the total dose and increasing the delivery accuracy [14]. As with the current investigation, the static phantom approach provides no information on the reproducibility of the target location, rather, it investigates the machine delivery reproducibility aspect.

An investigation into VMAT gating on a Versa HD (Elekta AB) was performed at the University of Iowa by Snyder et al. For the dose verification portion of their investigation, they measured decrements up to 9% for a gamma-index of 3%/3 mm when the gated plans were contrasted with the non-gated deliveries [20]. A single VMAT plan was recomputed for four energies (6 MV, 6 FFF, 10 MV, and 10 FFF) and the verification dose was measured to determine the reproducibility of gated delivery, and two patient plans were measured to evaluate the effect of the gating window length [20]. For verification plans with lower dose rate (6 MV and 10 MV) the gamma passing rates were comparable for non-gated and gated deliveries; however, increasing the dose rate (i.e. flattening filter free delivery) a marked decrease in the accuracy was observed. They also observed a decreased passing rate with large gating windows although small gating windows still had a decreased accuracy when compared with the ungated delivery. Because the large windows allow the gantry rotation speed to

be higher, the over-rotation is more severe. The gantry may not be in the required start position again and is forced to abruptly switch directions and resume treatment potentially decreasing the accuracy of large windows they hypothesize [20]. Slowing the gantry rotation speed, which can be achieved through several means, reduced the discrepancies noted for gated delivery.

Jermoumi et al. also evaluated the delivery accuracy of an Elekta linac on VMAT gating techniques. While Snyder et al. focuses on the delivery accuracy of large gating windows, Jermoumi et al. investigated small gating windows with similar approaches. They performed open field measurements with a static gantry position for a 20 x 20 cm^2 field to evaluate the gating accuracy [7]. With the 1%/1 mm gamma index criteria, gated open field measurements were within 2% with no statistical significance [7]. Using the commercial IBA MatriXX Evolution diode array (IBA Dosimetry) two lung SBRT VMAT plans were evaluated using beam-on: beam-off ratios of (1:3), (1.5:2.5), (2:2), and (3:1) and several beam-on times [14]. Gamma index criteria of 1% and 2% with 1 mm DTA was used for dosimetric comparisons. Using the 2%/ 1 mm gamma criteria, all VMAT plans had over 95% passing rates; however, 1%/ 1 mm passing rates were noticeably lower for the small (17%) gating window, only passing at 69.4% and 66.7% for the two respective cases, and all other cases had over 95% passing rates [7]. The significant decreases in passing rates with the small gating windows were due to the Elekta beam-on delay and delivery nature of the gantry and MLC leaf motions the authors concluded. A marked decrease in dosimetric accuracy was also observed for manually starting the beam from a beam-off state rather than resuming the beam from a beam-hold state attributed to differences in the electron gun going from a standby state to an active state vs. remaining in an active state [7]. Small gating windows should be avoided in order to maintain gating treatment accuracy.

A similar study was performed for gated treatments on a Varian TrueBeam linac

implemented with the Varian RPM system. Three VMAT SBRT plans were evaluated, all 10FFF, using the ArcCheck for dose distributions and an ionization chamber for point dose measurements. The 2%/ 2 mm gamma index was used to compare the dose distributions to the treatment planning system planned dose distribution for 100%, 50%, and 25% beam-on percentages. The authors measured average gamma passing rates of 86.1%, 86.0%, and 86.1% with point deviations of 1.2%, 1.1%, and 1.1% for 100%, 50%, and 25% beam-on times respectively [22]. Concluding that delivery over a wide range of gating windows is possible when carried out with a Varian TrueBeam and RPM system. Treatment times were also measured; the average treatment time increased from 74.3 seconds (100% beam-on) to 154.3 seconds and 347.9 seconds for the 50% and 25% beam-on times respectively [22]. PTV margins need to be weighed against the increased treatment times necessary with small gating windows.

Nicolini et al. performed a pre-clinical study evaluating respiratory-gated VMAT using RapidArc (Varian Medical Systems). The authors tested six, single arc VMAT plans under conditions of 2 Gy, 5 Gy, and 15 Gy per arc, with the two latter being of significance for stereotactic therapy [13]. Four gating windows, ungated, 30 second, 15 second, and 5 second beam-on times, were analyzed for the 2 Gy cases resulting in gating windows of 100%, 85%, 73%, and 68%, respectively. All 2 Gy/arc cases yielded 3%/ 3 mm gamma passing rates above 98%, and the authors noted substantial independence between various gating conditions with respect to 100% beam-on conditions [13]. To simulate stereotactic conditions, the authors tested plans of 5 Gy per arc with with 5 second beam-on window (68%) and 15 Gy per arc with 8 second beam-on window (70%). The 5 Gy plans were all above 98% passing rates for the 3%/ 3 mm gamma criteria; however, the 15 Gy plans, averaging approximately 45 beam interruptions, yielded passing rates 1-2% lower with the same criteria [13]. Still, all plans were above the clinically acceptable benchmark for approval. With a 70% gat-

ing window and 15 Gy per arc, treatment times averaged 6-7 minutes which is likely to lead to increased intra-fraction motion due to patient discomfort. The authors concluded VMAT gating may be accurately delivered using Varian linacs with the RPM system as the dosimetric agreement between the measured and planned doses were clinically acceptable.

Another group investigated gating on a Varian TrueBeam carried out with the RPM system. Qian et al. were specifically investigating a dose reconstruction technique from trajectory files of the TrueBeam system; however, they validated them using a phantom setup of the PTW Seven29 (PTW) ion chamber array [16]. With the array positioned between two 10 cm thick plastic water slabs, three patient VMAT plans (one double-arc 6 MV, one single-arc 10FFF, and one single-arc 15 MV) were evaluated for a 3 mm amplitude periodic motion breathing signal and a gating window of 25% to 70% [16]. Three period motion wavelengths were evaluated of 3, 4.5, and 6 seconds which translated into 1.4, 2.0, and 2.7 second beam-on periods, respectively. The authors observed passing rates of 99.8%, 100%, and 99.2%, respectively, when the 100% beam-on delivery was the reference for comparison using the 1%/ 1 mm gamma analysis for one patient case, and 100% passing rates for the other two patient cases [16]. The authors noted limitations of the study include: physical setup errors of the verification phantom, directional dependence corrections of the diode array are never perfect, and the artificial breathing pattern established by the phantom never mimics a clinical setting. The authors concluded dose verification using trajectory files of the TrueBeam system is a valid and effective method that can be applied for patient-specific QA. More importantly for the current investigation, they noted the TrueBeam can accurately realize gated VMAT plans through a variety of periodic respiratory periods, and the dosimetric accuracy of gated delivery, including that of several respiratory periods, is on par with the ungated delivery accuracy [16].

Park et al. created a novel approach to VMAT dose verification using roll-up ra-

diochromic film and dose analysis software [15]. With a two-body phantom consisting of an outer donut and an inner cylinder, radiochromic film was positioned in a groove between the bodies to allow for three-dimensional dose verification. In-house software was used to evaluate the planned two-dimensional dose distribution expected for the rolled-out film and measured film agreement. The authors evaluated three clinical VMAT cases (prostate, nasopharynx, and pelvic metastatic lesions). Park et al. achieved gamma pass ratios above 90% for the three plans evaluated with a 3%/3 mm DD/DTA criteria and a total dose error of less than 8.5% on the cylindrical surface [15]. They noted high dose errors in regions of steep dose gradients and with sections approaching organs at risk (OARs) [15]. To compensate the high dose regions, the authors evaluated the verification plans with a modified gamma analysis that yielded reasonable results in the region of interest. The use of radiochromic film in a cylindrical setup is advantageous because the film is flexible; nearly independent of dose rate, energy, and angular dependence; has high spatial resolution; and is practical; however, the advent of 2-D and 3-D diode arrays have largely replaced film dosimetry.

Tanooka et al. evaluated 3-D dose distributions on a spiral water phantom consisting of a main body filled with water and an acrylic holder for positioning the film; both the body and holder walls are 3 mm thick acrylic [21]. Nine prostate VMAT plans were delivered to the spiral phantom and the gamma analysis was performed to evaluate the agreement of the measured and planned dose distributions. Isodose profiles were also compared to the planned distribution and the measured distributions of the spiral phantom. Tanooka et al. reported a mean passing rate of 87% 3%/3 mm DTA/DD for a 2 mm dose grid that was increased to an average of 91.1% for a dose grid of 1 mm [21]. A smaller dose grid realizes the full potential of the high resolution capability of radiochromic film, and as demonstrated, yields higher passing rates for VMAT dose verification QA. The authors also reported that the

conventional 2-D gamma-index may not be appropriate in high-dose gradient regions due to setup uncertainties [21]. By using this method, dose measurement stability may be increased by eliminating the air gap between phantom materials and film. High spatial resolution and cost-effectiveness make the wrapped radiochromic film a viable alternative to diode arrays for patient plan verification.

1.4 Purpose

The purpose of this investigation was to investigate the use of small gating windows for radiotherapy treatments on a Varian Edge linear accelerator (linac). Small gating windows could potentially allow more accurate localization of the lesion because margins could be constricted; however, treatment accuracy may be limited by machine constraints. This investigation focuses on the machine limitations and further investigation will need to be carried out to determine the overall treatment accuracy using small gating windows with respect to clinical target coverage.

Chapter 2

Materials and Methods

All measurements were carried out on a Varian Edge Stereotactic linac equipped with an HD-MLC and Varian RPM system. Five clinically accepted VMAT plans were evaluated, each with five different beam-on windows, 100%, 70%, 50%, 30%, and 20%. Two of the plans were 6FFF and the other three were 10FFF. All treatment plans were created on the RayStation Treatment Planning System (RaySearch Laboratories); two of the plans consisted of co-planar overlapping arcs, while the other three were single arc plans, and they consisted of arcs between 170 degrees and 230 degrees of rotation.

2.1 Commercial QA Phantom

The ArcCHECK is a cylindrical patient specific QA phantom containing 1386 0.019 mm^3 diode detectors arranged in a helical grid to increase the sampling frequency and minimize the detector overlap as viewed from the beams eye view (BEV). Several inserts are available for the ArcCheck including the MultiPlug (Sun Nuclear Corporation) which was inserted for all measurements, that allows for ionization chamber dose measurements or planar film measurements. All ArcCheck measurements were analyzed with the SNC Patient Software (Sun Nuclear Corporation) that allows for DTA, gamma, and gradient compensation. Point doses were obtained with an Exradin A16 micro-ionization chamber (Standard Imaging) inserted into the Ar-

cCheck plug. A SuperMAX (Standard Imaging) electrometer collected the charge produced in the A16, and temperature and pressure corrections were applied to all point dose measurements. A Quasar Respiratory Motion Phantom (Modus Medical Devices Inc.) was used to provide a constant fifteen cycles per minute sinusoidal waveform for detection by the RPM system.

With the ArcCheck positioned at gantry isocenter, each plan was delivered with the five different beam-on configurations. The setup can be seen in Figure 2-1. All measured dose distributions were compared to the treatment planning system calculated dose distribution using the gamma and DTA analysis functions built into the SNC Patient software. The plan dose was recomputed on a 1 mm slice thickness CT of the ArcCheck phantom with 2x2x2 mm^3 dose grid. Point dose measurements were also compared with the planned isocenter dose calculated with RayStation. The standard deviaiton was also calculated as the error for each measurement.

Figure 2-1: Commercial phantom setup using the ArcCheck and Quasar.

2.2 Custom QA Phantom

Gafchromic EBT2 QD+ (International Specialty Products) was used for a second verification method. The phantom used can be seen in Figure 2-2; a complete setup is shown to the left, the top right displays a representative picture of the setup phantom, and the bottom right displays and axial CT image of the phantom. The radiochromic film scans were performed on an Epson Espression 10000XL (Epson America Inc.) flatbed scanner in professional mode using 24-bit color, 1200 dots per inch (dpi) and saved as .tif files.

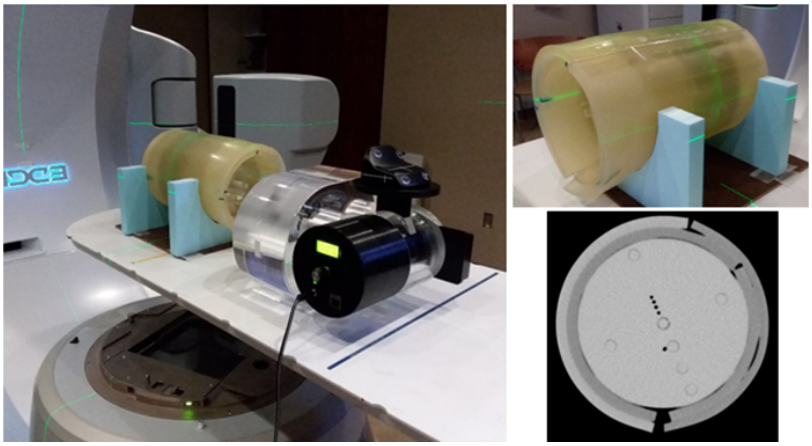

Figure 2-2: Custom acrylic QA phantom setup (Left), custom acrylic QA phantom (Top Right), axial CT of acrylic phantom (Bottom Right)

All films were scanned pre-irradiation and post-irradiation. Pre-irradiation film scans were used for film background subtraction and will be discussed later. The radiochromic film strips were wrapped around the cylindrical acrylic center followed by a single layer of plastic wrap to prevent the bolus from directly contracting the radiochromic film. Two centimeters (cm) of bolus was then wrapped around the acrylic center and taped into position. The five gating windows for each VMAT plan was then delivered to the wrapped radiochromic film with the beam isocenter

positioned at the film center in the superior-inferior direction. In an effort to increase the setup reproducibility, the base and mounts remained in the same position; the bolus wrapped acrylic cylinder was removed, re-wrapped, and repositioned. As a result, the table height and lateral position was able to remain constant, and the longitudinal position was shifted only to position the beam isocenter in the center of the film piece (as determined by the in-room laser system). The post-irradiation scans were performed following a 24 hour window to allow the film response to stabilize.

2.2.1 Dose Response Curve

A film dose response curve was created using 19 dose points ranging from 0 to 450 cGy in 25 cGy increments. Monitor unit settings were computed using RadCalc 6.2 (Lifeline Software Inc.). Square pieces of film, 4.5x4.5 cm^2, were positioned in the center of a 10x10 cm^2 field (at the surface) at 5.2 cm depth of tissue equivalent plastic. Backscatter was achieved with an acrylic slab of 5 cm thickness. A flattened 6 MV beam was used with max dose rate of 600 MU/min. Again, pre-irradiation and post-irradiation scans were performed for each piece of film, including a 24 hour period for response plateau in the post-irradiation film case.

Images were processed using an open source software where the pre-irradiation scan (background) was subtracted from the post-irradiation scan for each piece by alignment of the post-irradiation scan over the pre-irradiation scan and performing a subtraction. In order to achieve a monotonically decreasing response curve in RIT (Radiological Imaging Technology Inc.) the scans were inverted. The corrected files were then opened in RIT for the response calibration curve formation. A 1x1 cm^2 region of interest was positioned at the center of each piece yielding a mean pixel value for each scan and the dose was entered creating a plot of pixel value as a function of dose. The region of interest was carefully chosen to mimimize the standard deviation of the image volume used for the mean pixel value.

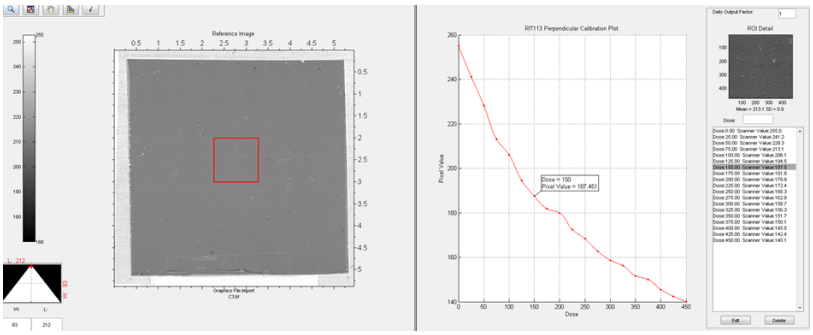

Figure 2-3: Film pice with ROI for mean pixel value (Left), calibration curve and list of dose points (Right).

2.2.2 Film Analysis

The SNC software takes DICOM RTDose and RTPlan files and calculates the expected dose each diode will receive from the given beam set. With the custom phantom, this is not possible; hence, a script had to be created to compute the dose along the circumference of the acrylic cylindrical phantom. A CT scan was obtained of the custom phantom using 1 mm slice thickness on a Bigbore CT (Phillips). The images were then imported into RayPhysics (RaySearch Laboratories). The acrylic center, outer bolus, and external contours were produced and density overrides were applied to the acrylic and bolus of 1.19 g/cm^3 and 1.06 g/cm^3 respectively. Upon phantom approval, QA plans were created on the phantom for each case and the script was ran to compute the dose along the outer acrylic surface to be used as the reference dose for absolute dose analysis.

VMAT plans were recomputed onto the custom acrylic phantom with a 2x2x2 cm3 dose grid. The script exported the dose as an ASCII file for import into RIT. The film images were co registered in the open source image processing software and scaled down to 25% of their original size and 300 dpi to allow RIT to handle the file size. The film measurement was loaded as the reference and analyzed with the red channel in order to maintain the high spatial resolution of the film rather than

accepting the lower TPS resolution; maintaining the high spatial resolution of the film comes at the expense of longer computation times for the gamma analysis in RIT. All five films for each case were registered using the same points to minimize the variance between each gating window and all were normalized to an area of intermediate dose exhibiting a small standard deviation (i.e. a low dose gradient). Figure 2-4 shows a single case reference and target dose distribution. The reference distribution was the radiochromic film measurement with the dose calibration curve applied analyzed using the red channel, and the target image was imported from the TPS as an ASCII file. The square seen in both images was the registration box in RIT where corresponding points can be identified an used to register the images together. Identical ROIs were placed around the high dose region to be used for analysis. Gamma analysis was performed through RIT using a 3%/3 mm criteria with a 10% low dose threshold to minimize the background noise. The fine tune registration feature was also selected to correct inherent errors in selecting the registration points.

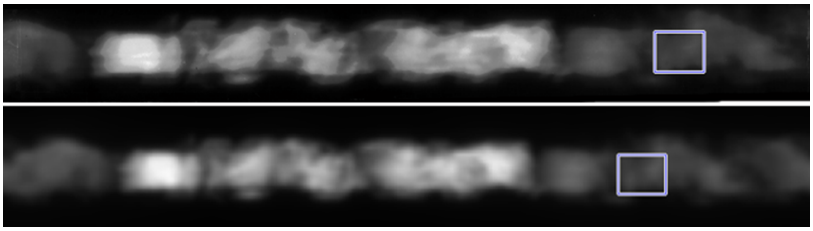

Figure 2-4: Reference dose distribution (radiochromic film) (Top), target dose distribtuion (TPS calculated) (Bottom).

Chapter 3

Results

3.1 Commercial Phantom

All gating windows had average 3%/3 mm gamma passing rates over 95% (typical clinically relevant passing rates) seen in Figure 3-1.

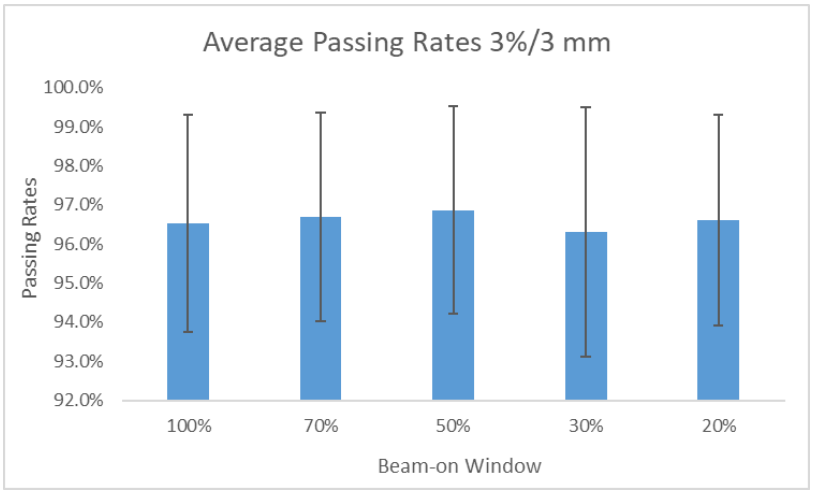

Figure 3-1: Average gamma passing rates for 3%/3 mm criteria with standard deviation error bars.

Figure 3-2 shows average gamma index of 1%/ 1 mm and 0.5%/ 0.5 mm, and dose difference of 1% passing rates for the five cases with the TPS planned dose distribution as the reference. Error bars represent the standard deviation of the five case measurements. No statistically significant decrease in gamma passing rates were

noted for either gamma index analysis or the DD of 1% through all gating windows.

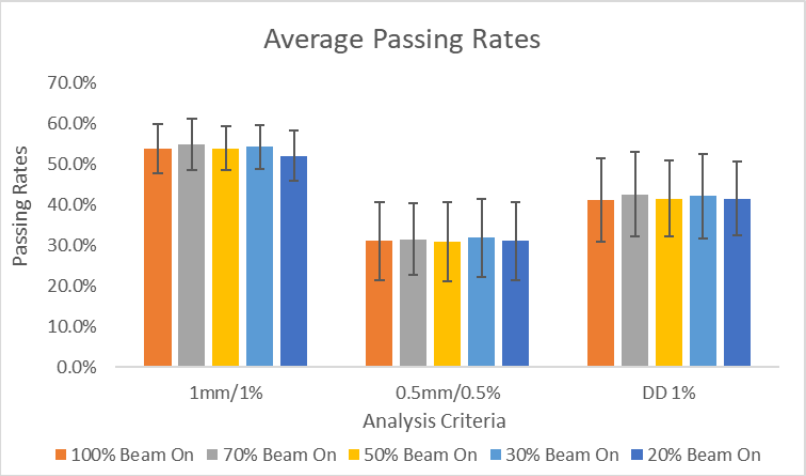

Figure 3-2: Average passing rates for 1 mm/ 1% gamma, 0.5 mm/ 0.5% gamma, and 1% dose difference

Absolute point deviation measurements with the A16 micro-ionization chamber showed considerable variation as seen in Figure 3-3; however, a notable increase in agreement with TPS calculated point deviation values was observed for the small gating windows. Maximum deviation from the TPS calculated point dose occurred for the gating window of 70% beam-on in case 5 and was the only point dose where the deviation was greater than 5%. Comparing each gating window to the 100% beam-on delivery, the maximum deviation was 2.1%, which occurred for a 20% beam-on window in case 4, but the average deviation from the 100% beam-on approach was only 0.2%.

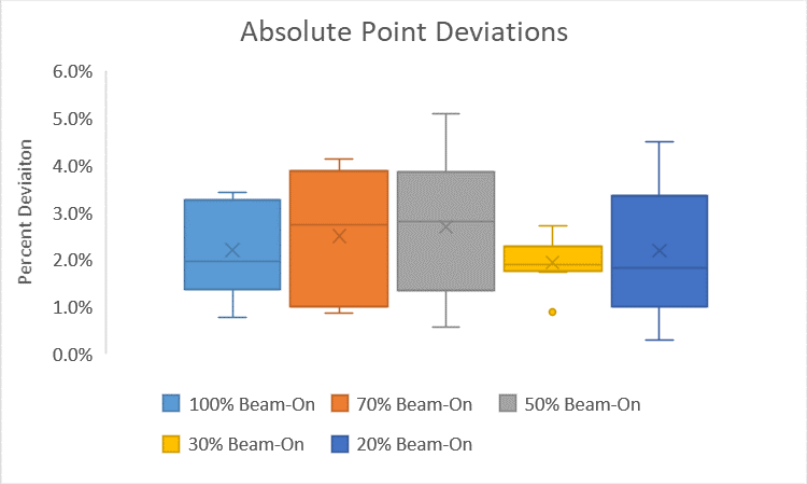

Figure 3-3: Absolute point deviations including outliers.

Each gating window was compared to the 100% beam-on delivery (100% beam-on was the reference) and is presented in Figure 3-4. While all passing rates were greater than 95%, a marked decrease in the passing rates were observed for the two small gating windows. While it appears there is a significant decrease in the delivery reproducibility with smaller gating windows, the deviation was entirely the result of two cases (three and four) for a 1% dose difference.

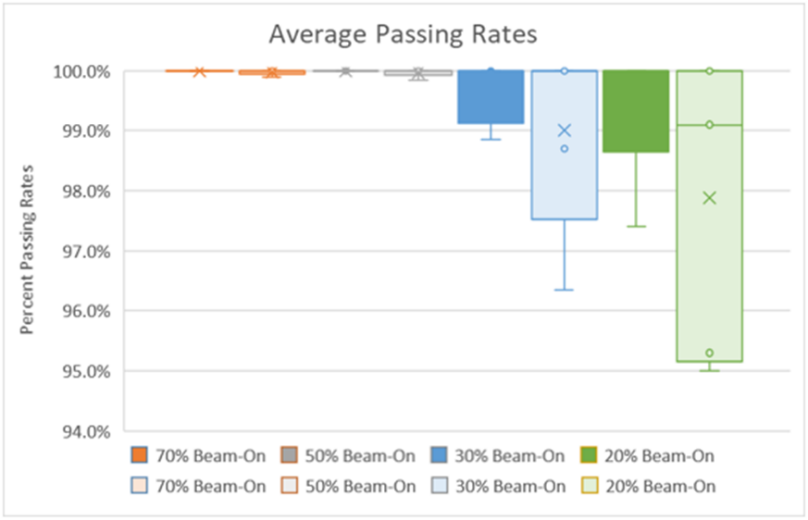

Figure 3-4: Average passing rates for dose difference of 1% and 0.5%. The reference for comparison was the 100% beam-on delivery.

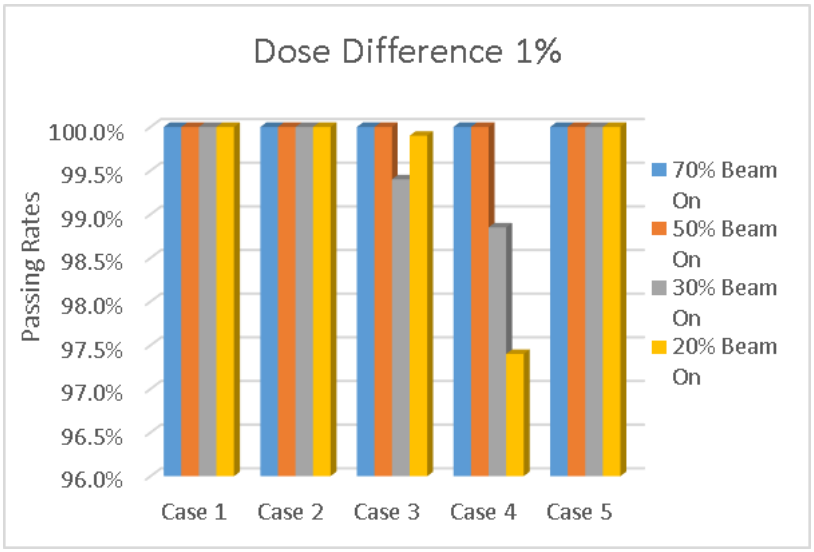

Figure 3-5: Dose difference of 1% for each case with the ungated delivery as the reference

With a 0.5% dose difference (Figure 3-6), the small gating window for case 5 contributes to the overall decrease in passing rates.

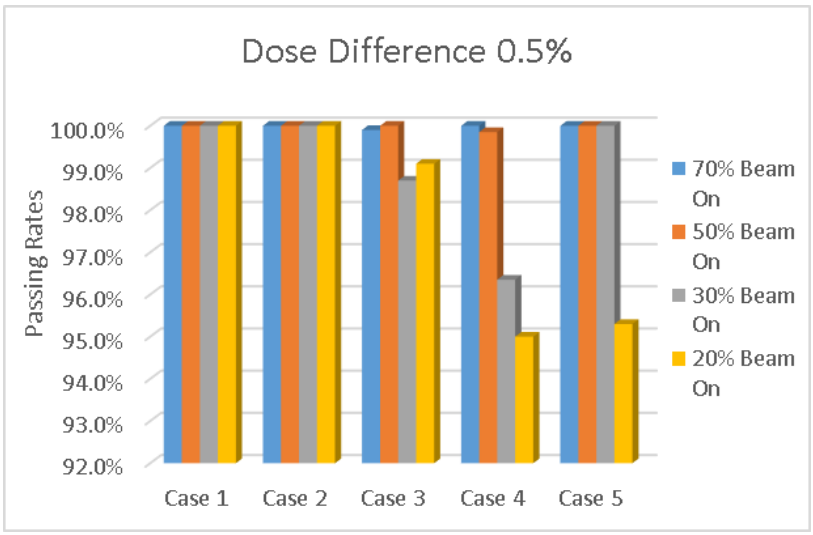

Figure 3-6: 0.5% dose difference with ungated delivery as the reference

3.2 Treatment Time

Average treatment times can be seen in Figure 3-7, and the fractional increase in treatment time for each gating window is presented in Table 3.1.

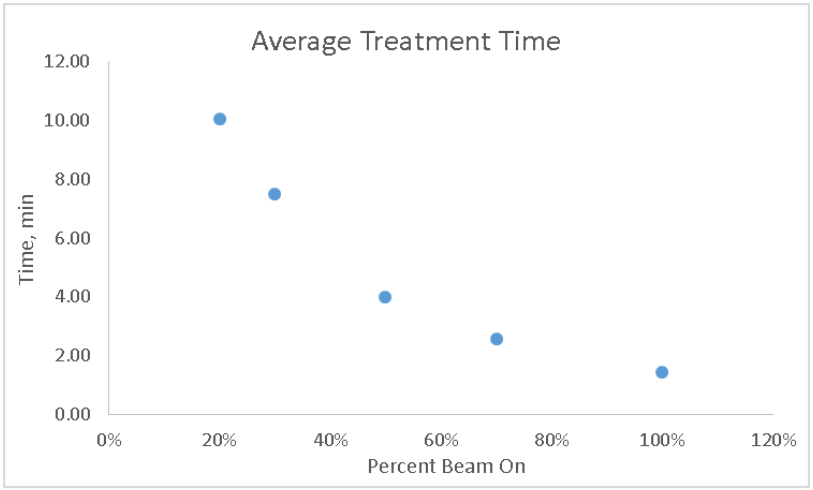

Figure 3-7: Average treatment times for various beam-on windows.

Table 3.1: Average fractional increase in treatment time.

Gating Window	Average Treatment Time, min	Fractional Increase
100%	1:26	-
70%	2:33	1.8
50%	4:00	2.8
30%	7:29	5.2
20%	10:03	7.0

The average treatment times listed only indicate that required to delivery the intended dose; it does not account for patient setup and pre-treatment imaging.

3.3 Custom Phantom

Figure 3-8 shows the average gamma passing rates for 3%/3 mm criteria for the radiochromic film wrapped around the custom acrylic cylindrical phantom and the gamma passing rates for each case can be seen in Figure 3-9. Finally, Figure 3-10 shows a line profile running the length of the film used for the gamma analysis.

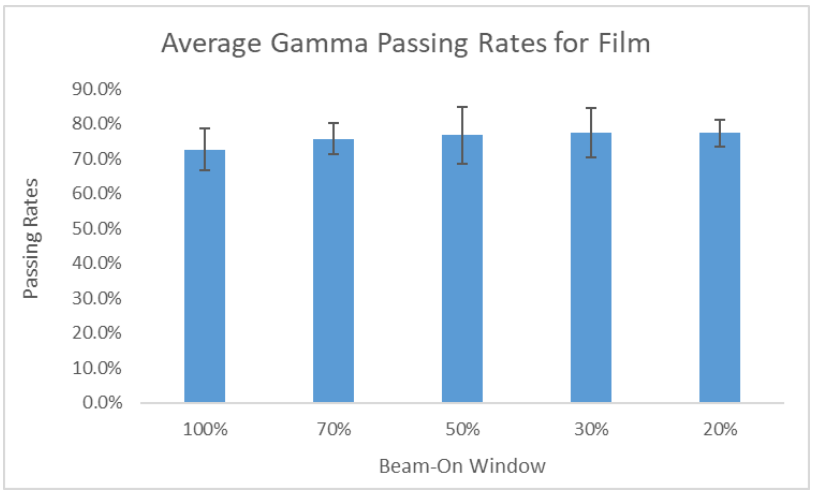

Figure 3-8: Average gamma passing rates for radiochromic film with standard deviation error bars.

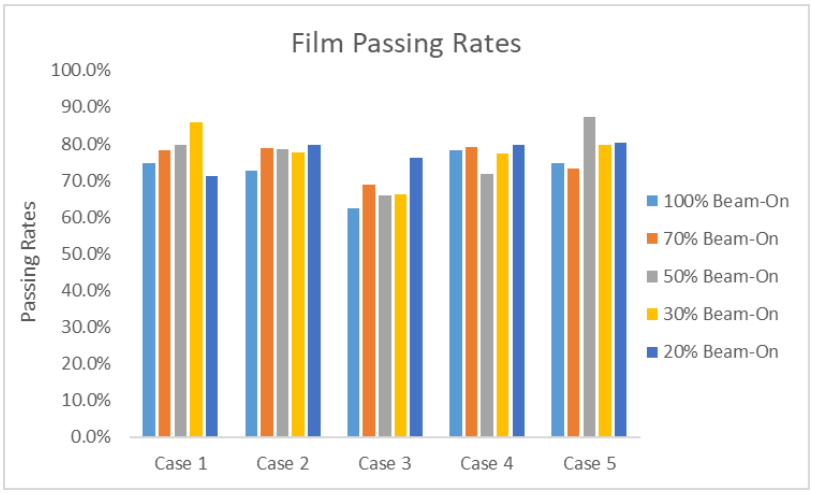

Figure 3-9: Radiochromic film gamma passing rates for each case and beam-on window.

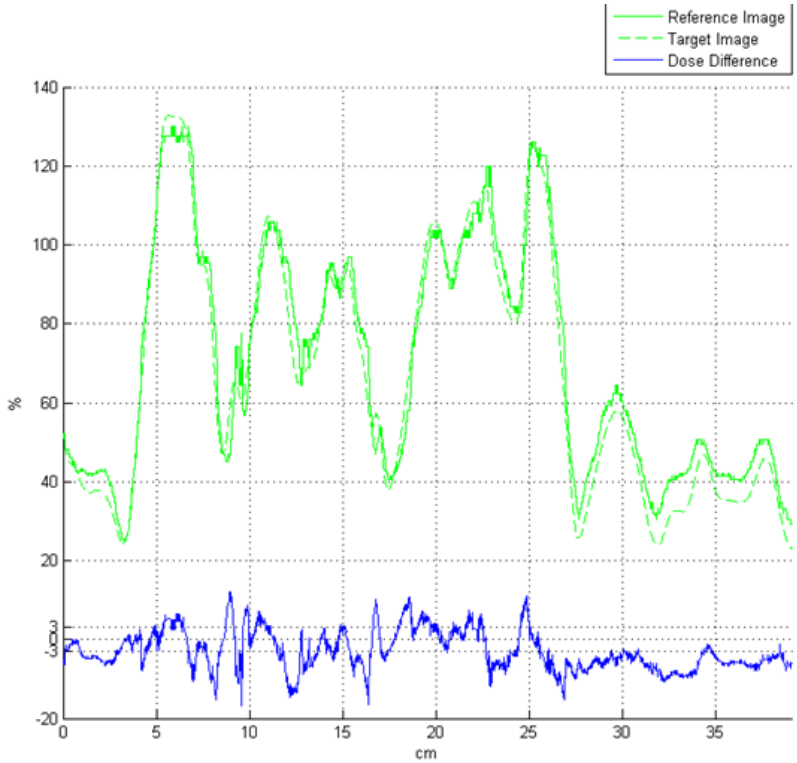

Figure 3-10: Line profile running the length of the radiochromic film for one case.

Chapter 4

Discussion

In theory, small gating windows allow for smaller PTVs because the motion over fewer phases is typically less. Intra-fraction motion; however, could negate this theoretical benefit. Treatment time is a major consideration that needs to be considered to try to assess the potential for intra-fractional motion. Comparison of the measured dose distribution to the TPS calculated dose distribution showed no statistical variation between different gating windows indicating small windows are effectively able to deliver the gated treatment. However, as seen in Figure 3-5 and Figure 3-6, there may be more to consider. It appears the small gating windows have a measurably decreased delivery accuracy compared to the 100% beam-on plans or plans implemented with large gating windows. Using the dose difference criteria, SNC Patient only analyzes the expected point and measures if it is within the dose difference criteria set. High dose gradients across the diode may significantly impact the analysis because it does not find a point within a set distance; more specifically, a slight shift in the dose gradient can result in significant deviations in the passing rates between the reference and target dose distributions. Although there is a notable decrease in passing rates when the gated delivery was compared to the ungated delivery, all passing rates, including the 0.5% dose difference rates, were above 95% and clinically acceptable. Caution must be exercised with the small gating windows and should be

evaluated on a case-by-case basis.

As seen in Figure 3-7 and Table 3-1, small gating windows yield significant increases in treatment delivery time as expected. With the patient laying on the couch longer, the likelihood of intra-fraction motion is significantly increased which would negate any dosimetric advantages intended with the small gating windows. Patient discomfort and quality of care is also of concern in this case. Accounting for patient setup and pre-treatment imaging, overall treatments times become prohibitive, especially for clinics with high patient loads due to limited machine availability.

The calibration curve for the radiochromic film was obtained with a 6 MV beam although the treatments plans were carried out with flattening filter free beams. There is relatively little energy dependence for radiochromic film over the typical mega voltage therapy range so there is little difference in response for beams of differing qualities [1]. The flattened beam allowed a uniform ROI to be selected exhibiting little standard deviation whereas the FFF beam will be forward peaked and suffer from a greater standard deviation over the ROI; smaller ROIs suffer from greater noise too. To limit the amount of errors that would be introduced through an automated image alignment software, the images were manually aligned for background subtraction. Unfortunately, the radiochromic film measurements needed to be normalized making the labor intensive background subtraction process less useful. Ideally, there would not have to be any normalization; the dose calibration curve would allow for close agreement of the measured dose distribution with the TPS planned dose. The higher spatial resolution of the film was not able to accurately distinguish between a high dose gradient error or the potential decreased delivery accuracy seen in Figure 3-5 or Figure 3-6, unfortunately. Ultimately, the film measurements did not show a statistically significant decrease in delivery accuracy of small gating windows for treatment.

As seen in Figure 2-2, there is some inherent setup uncertainty with the custom phantom. Ideally, an acrylic donut would be machined with a groove for the film to

be situated in that would slide over the cylindrical phantom securely. Bolus sheets needed to be fastened together while attempting to minimize air-gaps that can adversely affect the expected dose delivered. In the treatment planning system, the bolus 'shell' had a density override applied to minimize errors that would be introduced by dose computation with the air-gaps present and because setup can never be identical between different pieces of film. The density override also allowed one phantom CT to be imported into the TPS; during setup and film measurements, the large gap produced by taping the bolus slabs together was positioned where the film edges did not completely encompass the acrylic cylinder. The gap was also situated on the opposite side of the delivered arc. Because the largest arc was 230 degrees, the beam never entered through the gap securing the bolus slabs (i.e. it did not adversely effect the dose delivered to the radiochromic film).

Machine variability between deliveries was not taken into account with this study, specifically, delivery variability between successive plan deliveries with the same gating parameters. This could be investigated by taking several film measurements and determining if there is significant variability between deliveries using the same gating windows. Future studies investigating open field arc measurements could potentially yield valuable information on gated VMAT deliveries that would eliminate potential errors introduced by MLC positions in clinical treatment plans. Although dose rate as a function of gantry speed is evaluated on a monthly basis for QA purposes, future studies may also be valuable to ensure accurate gated delivery over the range of dose rates available. Snyder et al. found a marked decrease in delivery accuracy with high dose rates in combination with large gating windows [20]. They were able to reduce the maximum gantry rotation speed on the machine to reduce the effect; however, this is not a patient specific adjustment meaning the maximum rotation speed would be reduced for all deliveries. Another option they investigated, and implemented, involved decreasing the dose rate for gated deliveries which is plan specific [20].

Chapter 5

Conclusions

Small gating windows can lead to lower volumes of normal tissue receiving prescription dose because there is less lesion movement over a smaller fraction of the respiratory cycle. In turn, the frequency of normal tissue complications is decreased, and the potential for dose escalation with similar normal tissue complication probabilities becomes feasible.

Small gating windows showed no statistically significant decrease in passing rates when compared to the TPS calculated dose distribution suggesting there is minimal difference between 100% beam-on delivery and small gating windows. For a few cases, a decreased passing rate for small gating windows (less than 50%) was observed when the gating window was compared to 100% beam-on delivery. Gating windows smaller than 50% should be evaluated to ensure the small gating window gated delivery is clinically acceptable. Significant increases in treatment times accompany small gating windows which may lead to increased intra-fractional motion, patient discomfort, and potential scheduling conflicts, and the increased treatment time needs to be weighted against the potential dosimetric advantage of the small gating window.

More work needs to be done to assess the accuracy of dose delivery to a moving lesion with small gating windows as this study only investigated the delivery aspect. The amount of increased intra-fractional motion needs to be investigated to determine

the maximum treatment time that can be comfortably tolerated by a patient before the dosimetric advantage of the small gating window can no longer be realized.

References

[1] Bijan Arjomandy, Ramesh Tailor, Aman Anand, Narayan Sahoo, Michael Gillin, Karl Prado, and Milos Vicic. Energy dependence and dose response of gafchromic ebt2 film over a wide range of photon, electron, and proton beam energies. *Medical physics*, 37(5):1942–1947, 2010.

[2] James M Balter, Kwok L Lam, Cornealeus J McGinn, Theodore S Lawrence, and Randall K Ten Haken. Improvement of ct-based treatment-planning models of abdominal targets using static exhale imaging. *International Journal of Radiation Oncology Biology Physics*, 41(4):939–943, 1998.

[3] Gauthier Bouilhol, Myriam Ayadi, Simon Rit, Sheeba Thengumpallil, Joël Schaerer, Jef Vandemeulebroucke, Line Claude, and David Sarrut. Is abdominal compression useful in lung stereotactic body radiation therapy? a 4dct and dosimetric lobe-dependent study. *Physica Medica: European Journal of Medical Physics*, 29(4):333–340, 2013.

[4] Laura A Dawson, Kristy K Brock, Sahira Kazanjian, Dwight Fitch, Cornelius J McGinn, Theodore S Lawrence, Randall K Ten Haken, and James Balter. The reproducibility of organ position using active breathing control (abc) during liver radiotherapy. *International Journal of Radiation Oncology Biology Physics*, 51(5):1410–1421, 2001.

[5] Philippe Giraud and Annie Houle. Respiratory gating for radiotherapy: main technical aspects and clinical benefits. *ISRN Pulmonology*, 2013, 2013.

[6] William B Harms, Daniel A Low, John W Wong, and James A Purdy. A software tool for the quantitative evaluation of 3d dose calculation algorithms. *Medical physics*, 25(10):1830–1836, 1998.

[7] Mohammed Jermoumi, Roger Xie, Daliang Cao, David J Housley, and David M Shepard. Does gated beam delivery impact delivery accuracy on an elekta linac? *Journal of applied clinical medical physics*, 18(1):90–95, 2017.

[8] Paul J Keall, Gig S Mageras, James M Balter, Richard S Emery, Kenneth M Forster, Steve B Jiang, Jeffrey M Kapatoes, Daniel A Low, Martin J Murphy, Brad R Murray, et al. The management of respiratory motion in radiation oncology report of aapm task group 76. *Medical physics*, 33(10):3874–3900, 2006.

[9] Daniel A Low and James F Dempsey. Evaluation of the gamma dose distribution comparison method. *Medical physics*, 30(9):2455–2464, 2003.

[10] Daniel A Low, William B Harms, Sasa Mutic, and James A Purdy. A technique for the quantitative evaluation of dose distributions. *Medical physics*, 25(5):656–661, 1998.

[11] Moyed Miften, Arthur Olch, Dimitris Mihailidis, Jean Moran, Todd Pawlicki, Andrea Molineu, Harold Li, Krishni Wijesooriya, Jie Shi, Ping Xia, et al. Tolerance limits and methodologies for imrt measurement-based verification qa: Recommendations of aapm task group no. 218. *Medical physics*, 2018.

[12] Yoshiharu Negoro, Yasushi Nagata, Tetsuya Aoki, Takashi Mizowaki, Norio Araki, Kenji Takayama, Masaki Kokubo, Shinsuke Yano, Sachiko Koga, Keisuke Sasai, et al. The effectiveness of an immobilization device in conformal radiotherapy for lung tumor: reduction of respiratory tumor movement and evaluation of the daily setup accuracy. *International Journal of Radiation Oncology Biology Physics*, 50(4):889–898, 2001.

[13] Giorgia Nicolini, Eugenio Vanetti, Alessandro Clivio, Antonella Fogliata, and Luca Cozzi. Pre-clinical evaluation of respiratory-gated delivery of volumetric modulated arc therapy with rapidarc. *Physics in Medicine & Biology*, 55(12):N347, 2010.

[14] Kimiya Noto, Shinichi Ueda, Hironori Kojima, Naoki Isomura, Akihiro Takemura, Shigeyuki Takamatsu, Tomoyasu Kumano, and Tsuyoshi Takanaka. Accuracy of dose delivery in multiple breath-hold segmented volumetric modulated arc therapy: a static phantom study. *Journal of Radiotherapy*, 2014, 2014.

[15] Ji-Yeon Park, Jeong-Woo Lee, Kyoung-Sik Choi, Jung Seok Lee, You-Hyun Kim, Semie Hong, and Tae-Suk Suh. Development of a novel quality assurance system based on rolled-up and rolled-out radiochromic films in volumetric modulated arc therapy. *Medical physics*, 38(12):6688–6696, 2011.

[16] Jianguo Qian, Lei Xing, Wu Liu, and Gary Luxton. Dose verification for respiratory-gated volumetric modulated arc therapy. *Physics in Medicine & Biology*, 56(15):4827, 2011.

[17] Vincent M Remouchamps, Nicola Letts, Frank A Vicini, Michael B Sharpe, Larry L Kestin, Peter Y Chen, Alvaro A Martinez, and John W Wong. Initial clinical experience with moderate deep-inspiration breath hold using an active breathing control device in the treatment of patients with left-sided breast cancer using external beam radiation therapy. *International Journal of Radiation Oncology Biology Physics*, 56(3):704–715, 2003.

[18] Vincent M Remouchamps, Frank A Vicini, Michael B Sharpe, Larry L Kestin, Alvaro A Martinez, and John W Wong. Significant reductions in heart and lung doses using deep inspiration breath hold with active breathing control and intensity-modulated radiation therapy for patients treated with locoregional

breast irradiation. *International Journal of Radiation Oncology Biology Physics*, 55(2):392–406, 2003.

[19] Katharina E Sixel, Marianne C Aznar, and Yee C Ung. Deep inspiration breath hold to reduce irradiated heart volume in breast cancer patients. *International Journal of Radiation Oncology Biology Physics*, 49(1):199–204, 2001.

[20] Jeffrey E Snyder, Ryan T Flynn, and Daniel E Hyer. Implementation of respiratory-gated vmat on a versa hd linear accelerator. *Journal of applied clinical medical physics*, 18(5):152–161, 2017.

[21] Masao Tanooka, Hiroshi Doi, Hideharu Miura, Hiroyuki Inoue, Yasue Niwa, Yasuhiro Takada, Masayuki Fujiwara, Toshiyuki Sakai, Kiyoshi Sakamoto, Norihiko Kamikonya, et al. Three-dimensional radiochromic film dosimetry for volumetric modulated arc therapy using a spiral water phantom. *Journal of radiation research*, 54(6):1153–1159, 2013.

[22] T Tawonwong, S Suriyapee, S Oonsiri, T Sanghangthum, and P Oonsiri. The dose delivery effect of the different beam on interval in fff sbrt: Truebeam. In *Journal of Physics: Conference Series*, volume 694, page 012026. IOP Publishing, 2016.

[23] Yoichi Watanabe, Leighton Warmington, and N Gopishankar. Three-dimensional radiation dosimetry using polymer gel and solid radiochromic polymer: From basics to clinical applications. *World journal of radiology*, 9(3):112, 2017.

[24] Matthew Williams and Peter Metcalfe. Radiochromic film dosimetry and its applications in radiotherapy. In *AIP Conference Proceedings*, volume 1345, pages 75–99. AIP, 2011.

[25] John W Wong, Michael B Sharpe, David A Jaffray, Vijay R Kini, John M Robertson, Jannifer S Stromberg, and Alavro A Martinez. The use of active breathing

control (abc) to reduce margin for breathing motion. *International Journal of Radiation Oncology Biology Physics*, 44(4):911–919, 1999.

[26] Wouter Wunderink, Alejandra Mendez Romero, Willy De Kruijf, Hans De Boer, Peter Levendag, and Ben Heijmen. Reduction of respiratory liver tumor motion by abdominal compression in stereotactic body frame, analyzed by tracking fiducial markers implanted in liver. *International Journal of Radiation Oncology Biology Physics*, 71(3):907–915, 2008.